

TECHNICAL REPORT ARCCB-TR-96035

**SOME METHODS OF REPRESENTING FATIGUE LIFETIME AS  
A FUNCTION OF STRESS RANGE AND INITIAL CRACK SIZE**

**A. P. PARKER  
J. H. UNDERWOOD**

DECEMBER 1996



**US ARMY ARMAMENT RESEARCH,  
DEVELOPMENT AND ENGINEERING CENTER  
CLOSE COMBAT ARMAMENTS CENTER  
BENÉT LABORATORIES  
WATERVLIET, N.Y. 12189-4050**



APPROVED FOR PUBLIC RELEASE; DISTRIBUTION UNLIMITED

19970325 022

Y30 Q111772-4050

#### **DISCLAIMER**

The findings in this report are not to be construed as an official Department of the Army position unless so designated by other authorized documents.

The use of trade name(s) and/or manufacturer(s) does not constitute an official indorsement or approval.

#### **DESTRUCTION NOTICE**

For classified documents, follow the procedures in DoD 5200.22-M, Industrial Security Manual, Section II-19 or DoD 5200.1-R, Information Security Program Regulation, Chapter IX.

For unclassified, limited documents, destroy by any method that will prevent disclosure of contents or reconstruction of the document.

For unclassified, unlimited documents, destroy when the report is no longer needed. Do not return it to the originator.

# REPORT DOCUMENTATION PAGE

Form Approved  
OMB No. 0704-0180

Public reporting burden for this collection of information is estimated to average 1 hour per response, including the time for reviewing instructions, searching existing data sources, gathering and maintaining the data needed, and completing and reviewing the collection of information. Send comments regarding this burden estimate or any other aspect of this collection of information, including suggestions for reducing this burden, to Washington Headquarters Services, Directorate for Information Operations and Reports, 1215 Jefferson Davis Highway, Suite 1204, Arlington, VA 22202-4302, and to the Office of Management and Budget, Paperwork Reduction Project (0704-0180), Washington, DC 20503.

1. AGENCY USE ONLY (Leave blank)		2. REPORT DATE December 1996		3. REPORT TYPE AND DATES COVERED Final	
4. TITLE AND SUBTITLE SOME METHODS OF REPRESENTING FATIGUE LIFETIME AS A FUNCTION OF STRESS RANGE AND INITIAL CRACK SIZE				5. FUNDING NUMBERS AMCMS No. 6111.02.H611.1	
6. AUTHOR(S) A.P. Parker (Royal Military College of Science, Cranfield University, Swindon, UK) and J.H. Underwood					
7. PERFORMING ORGANIZATION NAME(S) AND ADDRESS(ES) U.S. Army ARDEC Benet Laboratories, AMSTA-AR-CCB-O Watervliet, NY 12189-4050				8. PERFORMING ORGANIZATION REPORT NUMBER ARCCB-TR-96035	
9. SPONSORING / MONITORING AGENCY NAME(S) AND ADDRESS(ES) U.S. Army ARDEC Close Combat Armaments Center Picatinny Arsenal, NJ 07806-5000				10. SPONSORING / MONITORING AGENCY REPORT NUMBER	
11. SUPPLEMENTARY NOTES Presented at the 28th National Symposium on Fatigue and Fracture, Saratoga, NY, 25-27 June 1996. Published in proceedings of the symposium.					
12a. DISTRIBUTION / AVAILABILITY STATEMENT Approved for public release; distribution unlimited.				12b. DISTRIBUTION CODE	
13. ABSTRACT (Maximum 200 words)  An analysis is developed which permits fatigue lifetimes of components with pre-existing crack-like defects to be represented by a single expression which is a function of stress range and initial defect size; this is designated the Fatigue Intensity Factor (FIF). A graphical representation indicates that all such failures will fall upon a single, flat surface. The conventional S-N curve is shown to be a special case of this surface. Outliers from this surface may indicate deficiencies in estimates of stress range, of initial crack length, or that the failure is not due solely to fatigue. An equivalent analysis based upon the concept of threshold stress intensity indicates that a second, flat, intersecting surface exists. The conventional 'fatigue limit' often shown on S-N plots is shown to be a special case of this surface. Existing experimental data are used to define the surface, and examples of its application to the ordering of several potential fatigue failure locations within a single system and to interpreting non-standard fatigue failure are described.					
14. SUBJECT TERMS Fracture, Fatigue, Fatigue Intensity, Fatigue Lifetime, Stress Range, Stress Intensity, Stress Intensity Threshold, Crack Size, S-N curve				15. NUMBER OF PAGES 15	
				16. PRICE CODE	
17. SECURITY CLASSIFICATION OF REPORT UNCLASSIFIED	18. SECURITY CLASSIFICATION OF THIS PAGE UNCLASSIFIED	19. SECURITY CLASSIFICATION OF ABSTRACT UNCLASSIFIED	20. LIMITATION OF ABSTRACT UL		

## TABLE OF CONTENTS

	<u>Page</u>
INTRODUCTION .....	1
ANALYSIS .....	1
POSSIBLE APPLICATIONS .....	6
A PRESENTATION WHICH ENCOMPASSES ALL STEELS .....	7
EFFECT OF FATIGUE LIMIT .....	8
EXPERIMENTAL EVIDENCE AND EXAMPLES .....	9
SUMMARY AND CONCLUSIONS .....	13
ACKNOWLEDGEMENT .....	13
REFERENCES .....	14

### TABLES

1. Summary of Fatigue Life Information for Various Cannon Tubes .....	10
2. Summary of Stress Range Calculations .....	11

### LIST OF ILLUSTRATIONS

1(a). Schematic Representation of Typical $da/dN$ versus $\Delta K$ Plot .....	2
1(b). Conventional Lifetime Plot Showing Slope .....	2
2. 3D Fatigue Lifetime 'Surface' .....	4
3. Family of Conventional Lifetime Plots Relating to Different Initial Crack Sizes .	4
4. Single Line Plot of Lifetime for all Initial Crack Lengths .....	5
5. Potential Fatigue Failure Locations in a Gun Tube .....	6
6. Schematic of Single Line Plot Used to Assess Location 'Criticality' .....	7

7.	Straight Line Plot Presentation for all Steels .....	8
8.	Intersection of Fatigue Limit and Fatigue Lifetime Surfaces .....	9
9.	Fatigue Life as a Function of Stress Range and Initial Crack Size .....	12

## INTRODUCTION

Gun tubes develop bore cracks very early in their lifetime as a result of fatigue loading and severe thermal conditions that can cause so-called 'heat-checking'. There are also other potential failure locations, e.g. external notches and holes cut through the tube wall. It is important to have a clearly defined, well understood and easily presented design methodology to assess such potential failure locations and to identify the most critical.

Fatigue crack growth rates and associated lifetimes of components which contain pre-existing crack-like defects are frequently represented on a plot of  $\log da/dN$  (crack growth per loading cycle) versus  $\log \Delta K$  (Positive Stress intensity factor range). A typical relationship between these two parameters is shown in Fig. 1(a). Much of a component's lifetime falls within region B, which can be represented by Paris' law, [1], as:

$$\frac{da}{dN} = C(\Delta K)^m \quad (1)$$

where  $C$  and  $m$  are determined experimentally. In the case of steels  $m$  is typically 3.

The more traditional representation of Fatigue lifetime as a function of stress range is via a plot of  $\log$  (stress range) versus  $\log$  (cycles to failure), the 'S-N curve'. Results for tests on components (such as welded joints) which contain pre-existing defects are generally of the form shown in Fig. 1(b). Maddox [2] has demonstrated that the slope of the line in the traditional S-N presentation is equal to  $(-1/m)$ . Maddox includes an analysis, based upon Paris Law, retaining the full lifetime dependency upon initial and critical defect size and shape factor in order to develop a generalized effective stress range parameter. The purpose of this paper is to confine Maddox's analysis to variations of stress range and initial crack size, to produce graphical representations and to test their viability by comparing to existing experimental data relating to gun tubes.

## ANALYSIS

Assume an edge or center-cracked geometry with remotely applied uniaxial elastic stress range,  $\Delta\sigma^*$ . Hence the stress intensity factor range,  $\Delta K$ , for cracks small relative to the specimen width is given by:

$$\Delta K = Q\Delta\sigma^* \sqrt{\pi a} \quad (2)$$

where  $Q = 1$  for a straight-fronted center crack and 1.12 for an edge crack.

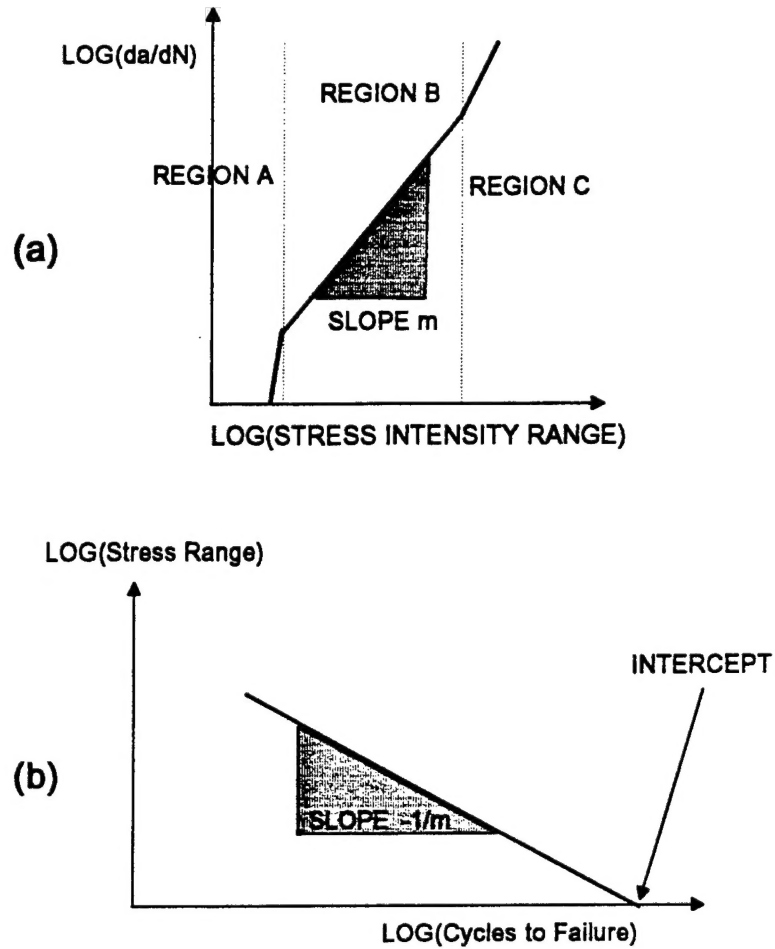


**Fig. 1 : (a) Schematic Representation of Typical  $da/dN$  versus  $\Delta K$  Plot**  
**(b) Conventional Lifetime Plot Showing Slope (related to Paris' exponent) and Intercept (related to initial Crack length)**

Using Paris' Fatigue crack growth Law, Eqn. (1), defining  $Q\Delta\sigma^*$  as  $\Delta\sigma$  and substituting (2) into (1) and integrating between initial crack length  $a_i$  and final crack length  $a_c$ , for constant amplitude cyclic loading:

$$N = \int_{a_i}^{a_c} \frac{da}{C(\Delta\sigma\sqrt{\pi a})^m} = \left[ \frac{a^{(1-m/2)}}{C\pi^{m/2}(1-m/2)(\Delta\sigma)^m} \right]_{a_i}^{a_c} \quad (3)$$

$$N = \frac{1}{C\pi^{m/2}(1-m/2)(\Delta\sigma)^m} \left[ a_c^{(1-m/2)} - a_i^{(1-m/2)} \right] \quad (4)$$

Eqn. (4) is the basis of the work by Maddox to relate Paris' law to the conventional log(stress range) versus log(Lifetime), 'S-N', presentation. Recognising that the square bracket is a constant for fixed initial crack size and  $a_c \gg a_i$  and taking logs of both sides leads to:

$$\log(N) = A - m\log(\Delta\sigma) \quad (5)$$

where A is a constant, or

$$\log(\Delta\sigma) = B - \left[ \frac{1}{m} \right] \log(N) \quad (6)$$

where B is a constant.

Eqn. (6) may be plotted in the conventional S-N fashion as shown in Fig. 1(b), and it gives the familiar negative slope relationship. Maddox noted that this slope is the negative reciprocal of the Paris law exponent, m. However, if Eqn. (4) is simply modified to embody  $a_c \gg a_i$  so that the effect upon lifetime of  $a_c$  is negligible (an assumption which generally alters lifetime by 5% or thereabouts), we obtain:

$$N = \frac{a_i^{(1-m/2)}}{C\pi^{m/2}(m/2-1)(\Delta\sigma)^m} \quad (7)$$

Which, on taking logs, produces:

$$\log N = -m\log \Delta\sigma + (1 - m/2)\log a_i - \log \{C\pi^{m/2}(m/2 - 1)\} \quad (8)$$

or alternatively:

$$\log \Delta\sigma = (-1/m)\log N + (1/m - 1/2)\log a_i - (1/m)\log \{C\pi^{m/2}(m/2 - 1)\} \quad (9)$$

Eqn. (8) indicates that a three-dimensional lifetime 'surface' exists, based upon axes  $\log N$ ,  $\log \Delta\sigma$  and  $\log a_i$ , see Fig. 2.



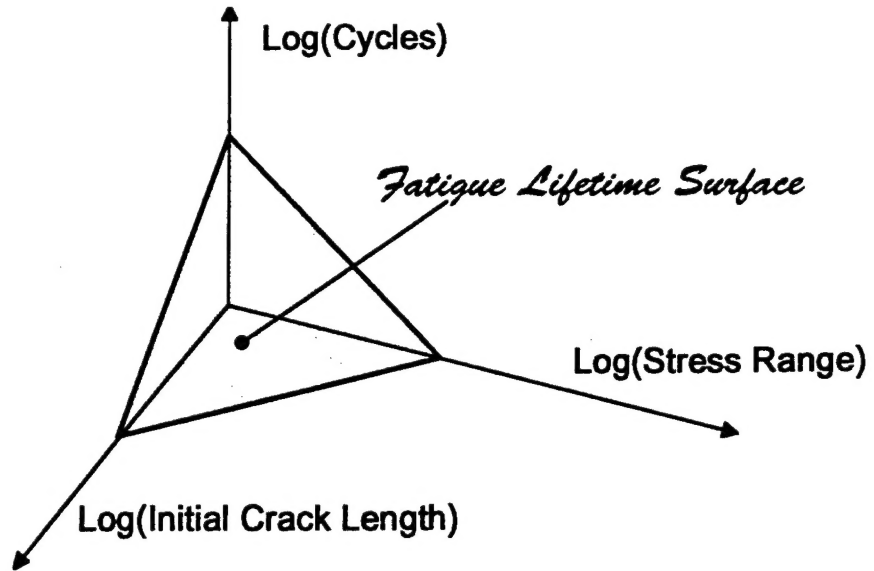


**Fig. 2 : 3D Fatigue Lifetime 'Surface'**

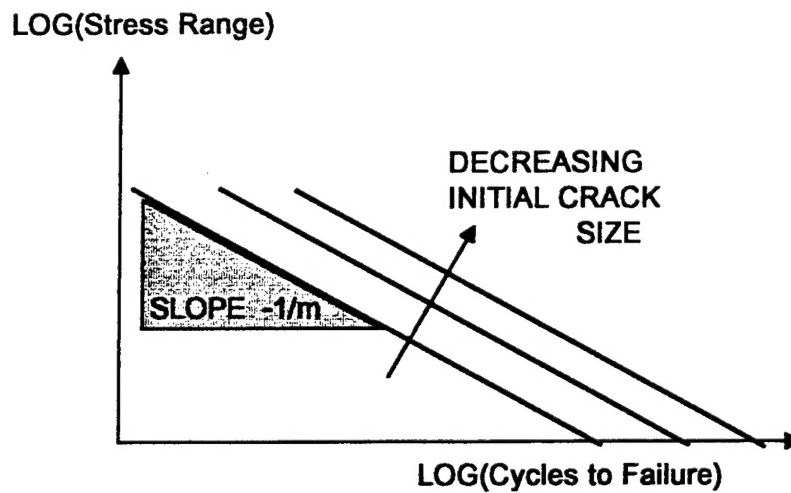


**Fig. 3 : Family of Conventional Lifetime Plots Relating to Different Initial Crack Sizes**

Eqn. (9) indicates the slope of the conventional 'S-N' plot; when viewed in the  $\log N$ ,  $\log \Delta \sigma$  plane this becomes a series of parallel lines with slope  $(-1/m)$ , see Fig. 3. Each line relates to a different value of initial crack size.

It is also possible to quantify the intercepts in Figures 2 and 3. From Eqn. (8), extrapolating to  $\log \Delta\sigma = 0$  gives the value of the intercept as:

$$\log N = (1 - m/2)\log a_i - \log \{C\pi^{m/2}(m/2 - 1)\} \quad (10)$$

alternatively extrapolating to  $\log a_i = 0$  gives:

$$\log N = -m\log \Delta\sigma - \log \{C\pi^{m/2}(m/2 - 1)\} \quad (11)$$

It is possible to force all results to fall on a single line by rearranging (9) to give:

$$\log \Delta\sigma + (1/2 - 1/m)\log a_i = -(1/m)\log N - (1/m)\log \{C\pi^{m/2}(m/2 - 1)\} \quad (12)$$

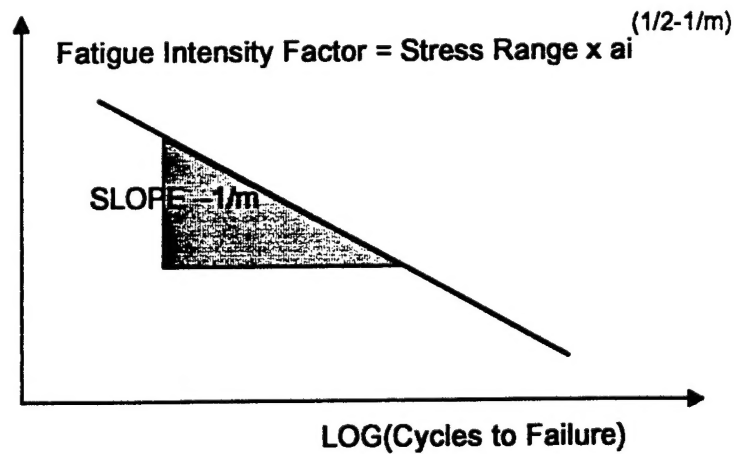
or

$$\log [\Delta\sigma \cdot a_i^{(1/2-1/m)}] = -(1/m)\log N - (1/m)\log \{C\pi^{m/2}(m/2 - 1)\} \quad (13)$$

It is convenient to define the Fatigue Intensity Factor (FIF) as:

$$\text{Fatigue Intensity Factor (FIF)} = \Delta\sigma \times a_i^{(1/2-1/m)} \quad (14)$$

LOG(Fatigue Intensity Factor)



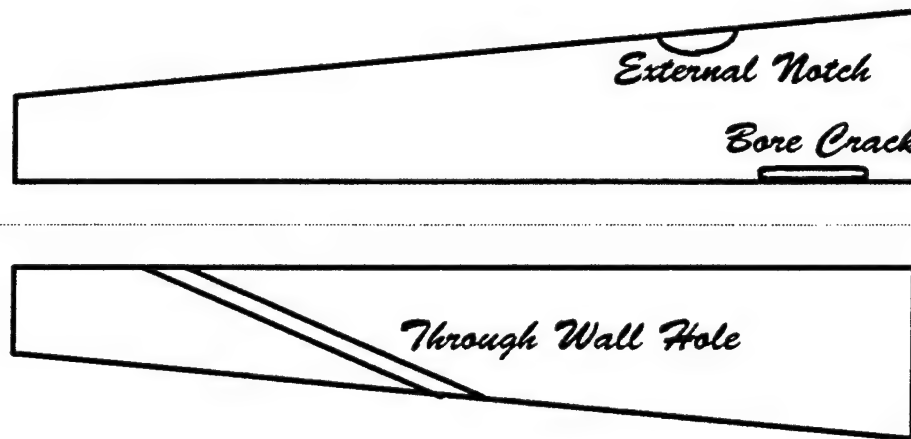
**Fig. 4 : Single Line Plot of Lifetime for all Initial Crack Lengths**

Fig. 4 shows a plot of the left hand side of Eqn. (13) versus  $\log N$ . Note that the last term on the right hand side is a material constant.

## POSSIBLE APPLICATIONS

Somewhat surprisingly, if a single data point is plotted as in Fig. 4 and Paris' coefficient and exponent are known, it is possible to extrapolate to the  $\log N$  axis and hence to calculate a value of  $a_i$ . Obviously such a procedure would be applied only when a significant number of data points was available.

The method of presentation employed in Fig. 4 makes possible a single line 'criticality' plot for a component or system which consists of a single material. In the case of a gun tube, for example, it is possible to plot each potential failure location and associated manufacturing process (such as the inclusion or exclusion of autofrettage) in order to assess the current and potential future critical fatigue failure locations.



**Fig. 5 : Potential Fatigue Failure Locations in a Gun Tube**

Fig. 5 shows, schematically, potential fatigue failure locations in a typical gun tube. Each location may be assessed for initial defect size and cyclic stress range (taking account of residual stress contributions, in particular the presence or absence of autofrettage). These values, when plotted against the axes defined in Fig. 4, will produce a series of points as illustrated in Fig. 6, all of which should fall on a straight line. Any outliers from such a plot either indicate an error in stress range (perhaps due to incorrect assessment of residual stress or to incorrect assessment of stress concentration), in initial defect size, or that the failure is due to other factors in addition to conventional mechanical fatigue.

LOG(Fatigue Intensity Factor)

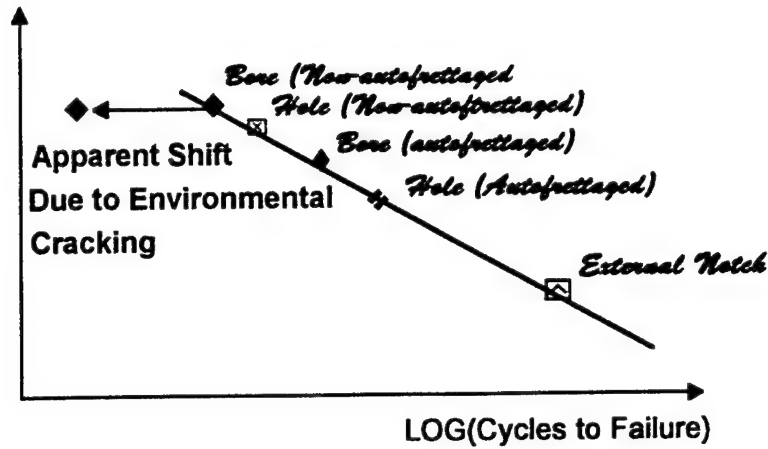


**Fig. 6 : Schematic of Single Line Plot Used to Assess Location 'Criticality'**

A possible outlier scenario related to environmental cracking is illustrated schematically.

#### A PRESENTATION WHICH ENCOMPASSES ALL STEELS

Thus far the Paris' law exponent ( $m$ ) and coefficient ( $C$ ) have been regarded as independent of one another. In the case of steels there is strong experimental evidence, for a range of microstructures, that  $C$  can be expressed as a function of  $m$ . Ref. [3], Chapter 2 indicates a simple relationship between  $C$  and  $m$  for steels, valid over the range  $m=1.8$  to  $m=4$ , namely:

$$C = \frac{1.315 \times 10^{-4}}{(895.4)^m} \quad \text{for crack growth in mm/cycle and } \Delta K \text{ in } \text{Nmm}^{-3/2} \quad (15)$$

Converting units this provides (see [3], Appendix 3)

$$C = \frac{1.315 \times 10^{-7}}{(28.3175)^m} \quad \text{for crack growth in m/cycle and } \Delta K \text{ in } \text{MNm}^{-3/2} \quad (16)$$

Hence, substituting from Eqn. (16) into Eqn. (13):

$$\begin{aligned} \log \left[ \Delta \sigma_i a_i^{(1/2 - 1/m)} \right] \\ = -(1/m) \log N - (1/m) \log \left\{ \left[ \frac{1.315 \times 10^{-7}}{(28.3175)^m} \right] \pi^{m/2} (m/2 - 1) \right\} \end{aligned} \quad (17)$$

Plotting this relationship in the same way as Fig. 4 leads to a set of straight lines, slope  $(-1/m)$ , as illustrated in Fig. 7 for the cases  $m=2.5$ , 3.0 and 3.5. Note that there is comparatively little difference between the three cases.

LOG(Fatigue Intensity Factor)

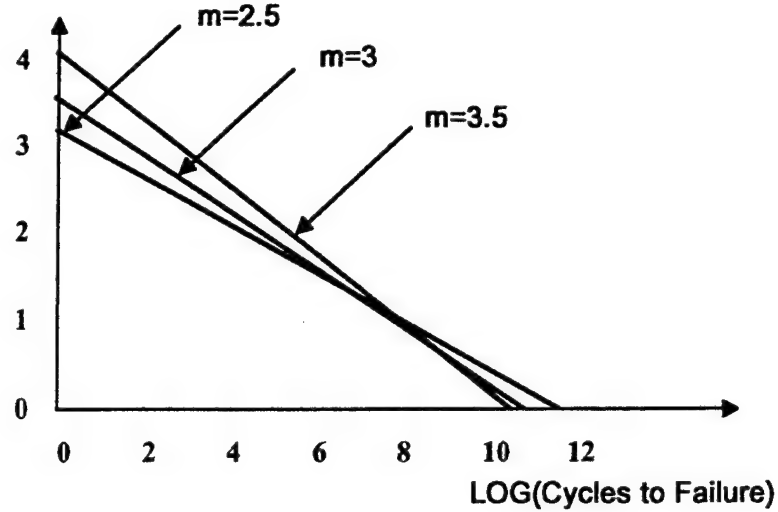


*Fig. 7 : Straight Line Plot Presentation for all Steels*

#### EFFECT OF FATIGUE LIMIT (STRESS INTENSITY RANGE THRESHOLD)

In the traditional (S-N) presentation for many materials there exists a so-called 'fatigue limit', i.e. a stress range below which the fatigue lifetime is infinite. The direct equivalent of this concept in conventional fracture and fatigue terms is a threshold value of stress intensity factor range,  $\Delta K_{th}$ , [3], below which small crack-like defects will not grow under cyclic loading.

In order to define a Fatigue Limit 'surface' in  $\log N - \log \Delta \sigma - \log a_i$  space for inclusion in a manner similar to Fig. 3 it is convenient to convert directly from Fracture/Fatigue to S-N presentation, retaining relevant parameters.

Since, at the Fatigue Limit:

$$\Delta \sigma \sqrt{\pi a_i} = \Delta K_{th} \quad (18)$$

taking logs

$$\log \Delta \sigma = \log(\Delta K_{th} / \sqrt{\pi}) - \log a_i \quad (19)$$

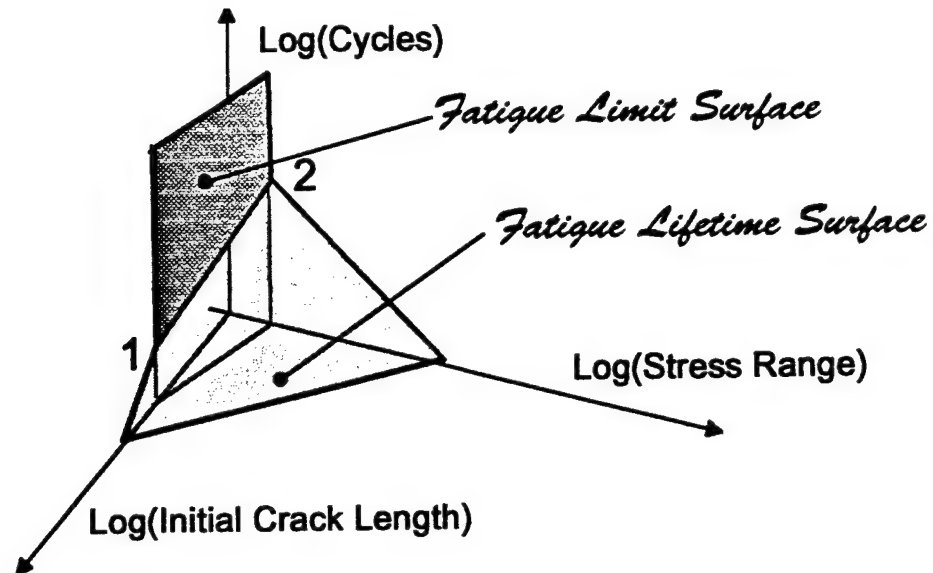


**Fig. 8 : Intersection of Fatigue Limit and Fatigue Lifetime Surfaces**

where the first term on the right hand side is a material constant.

Hence we see that we have defined a fatigue-limit 'surface' which lies parallel to the  $\log N$  axis and intersects the lifetime surface along the straight line, 1 - 2, Fig. 8. This fatigue limit 'surface' may be defined in one of two ways:

a. **Via a conventional S-N curve.** A single value of the fatigue limit for any stress range permits the full definition of the fatigue limit 'surface'. Again we note a somewhat surprising result. Recall that it was noted earlier that initial crack length may be calculated from a single S-N point, via the intercept. In this case the initial crack size and the stress range at the fatigue limit onset are sufficient to define  $\Delta K_{th}$ ; hence it is not necessary to undertake precise crack length observations to determine  $\Delta K_{th}$ .

b. **Via Fracture/Fatigue.** A known value of  $\Delta K_{th}$  is sufficient to define the surface.

## EXPERIMENTAL EVIDENCE AND EXAMPLES

The critical fatigue failure location within a cannon tube can vary depending upon the initial defect sizes, stress concentration effects of notches and holes, and the presence or absence of residual stress, typically due to autofrettage of the tube. Existing fatigue life test results from cannon tubes are available that can be used to demonstrate how well the fatigue intensity factor

concept of Fig. 4 works in describing fatigue life for the various conditions mentioned above. Table 1 summarizes fatigue results from early and recent work, [4, 5 and 6].

The cannon tubes had various inner and outer radii and values of applied pressure, but the comparison was limited to tubes of the same type of high strength steel with yield strength of about 1200 MPa. Some of the tubes contained residual stresses due to autofrettage which, in the case of the plated bore and through-wall hole results, had an effect on fatigue life. The effects of applied and residual stress on fatigue life were determined by the following calculation of stress range:

$$\Delta\sigma = k_T [\sigma_P + \sigma_R] + P_{\text{hole}} + P_{\text{crack}} \quad (20)$$

**Table 1 - Summary of Fatigue Life Information for Various Cannon Tubes**

	Inner Rad r1 mm	Outer Rad r2 mm	Yield Strngth $\sigma_Y$ MPa	Applied Pressure P MPa	Residual Stress $\sigma_R$ MPa	Stress Range $\Delta\sigma$ MPa	Initial Crack $a_i$ mm
Bore; fired	89	187	1250	345	0	890	0.50
Bore; unfired	89	187	1280	345	0	890	0.01
Bore; plated	89	142	1230	393	ID : -570	720	0.12
Thru-wall	53	76	1240	207	0	2210	0.01
	60	94	1170	297	ID : -460	2250	0.01
	78	107	1220	83	ID : -360	830	0.01
External Notch	78	142	1240	393	OD : +560	1200	0.01
							0.03

where  $k_T$  is the stress concentration factor of the through hole or the external notch,  $\sigma_P$  and  $\sigma_R$  are the applied and residual hoop stresses determined from the well known expressions for pressure vessels [7, 8], and  $P_{\text{hole}}$  and  $P_{\text{crack}}$  are the values of pressure that are applied to the inner surfaces of the through-hole and the growing crack, respectively. This implies, as before, that only the positive part of the stress range is included.

The values of the various parameters used to calculate  $\Delta\sigma$  are listed in Table 2. The values of  $k_T$  are the usual 3.0 for the through wall holes and 3.3 for the external notch, calculated from [7]:

$$k_T = 1 + 2a/b \quad (21)$$

where  $a$  is the depth (7.6 mm) of the semi-elliptically shaped external notch and  $b$  is the half-width of the notch (6.7 mm). Regarding residual stresses, the chromium plated tubes were the only bore-initiated failure in which the tubes had a residual stress at the bore. This compressive stress lowered considerably the stress range and greatly extended the fatigue life over that which would have been measured with no autofrettage residual stress. Other than this, no residual stresses were directly used in the stress range calculations. Residual stresses were present in two of the three types of through-wall hole tests, but, as has been shown in [6], the residual stress causes the crack initiation site to move to a point near mid-wall thickness where the residual stress is zero and the applied stress is reduced. Thus the residual stresses indirectly cause an extension of fatigue life at the new initiation site, which has been used in the  $\Delta\sigma$  calculation. Tensile residual stresses were present in the area of the external notch but were not considered because they did not add to the stress range. Finally, regarding pressure in the holes and cracks, note that the applied pressure has been added to the stress range as appropriate for the tube configuration and failure location.

**Table 2 - Summary of Stress Range Calculations**

	Stress conc. $k_t$	Applied Stress $\sigma_p$ MPa	Residual Stress $\sigma_R$ MPa	Pressure in hole $P_{hole}$ MPa	Pressure in Crack $P_{Crack}$ MPa
Bore; fired	1.0	547	0	n/a	345
Bore; unfired	1.0	547	0	n/a	345
Bore; plated	1.0	902	-547	n/a	393
Thru-wall					
$R_1 = 53\text{mm}$	3.0	599	0	207	207
$R_1 = 60\text{mm}$	3.0	552	0	297	207
$R_1 = 78\text{mm}$	3.0	221	0	83	83
External Notch	3.3	361	0	n/a	n/a

The fatigue life results based on Eqn. (20) and Tables 1 and 2 are shown in Fig. 9, using the type of single line plot in Fig. 4. The exponent of  $a_1$  is  $1/6$ , for the case here of  $m = 3$ . The fatigue lives,  $N$ , were measured from full size cannon tubes which had been fired several hundred times prior to hydraulic testing, except as noted, and then hydraulically pressure cycled to failure in the laboratory. The stress range calculations have been discussed above. The initial crack size of 0.01 mm, from recent work [6], was used for most of the tests here,



as a reasonable estimate of the inclusion size of the steel used in the tests, or alternatively, as an estimate of the roughness of the machined surface. In three cases metallographic measurements showed that  $a_i$  was larger than 0.01 mm. For the fired tubes with bore failure, heat check cracks of about 0.50 mm deep were observed. For the chromium plated tubes with bore failure, the cannon firing caused cracks in the plate to a depth equal to the plate thickness, 0.12 mm. For one of the externally notched tubes a rapid machining process resulted in an  $a_i$  of about 0.03 mm.

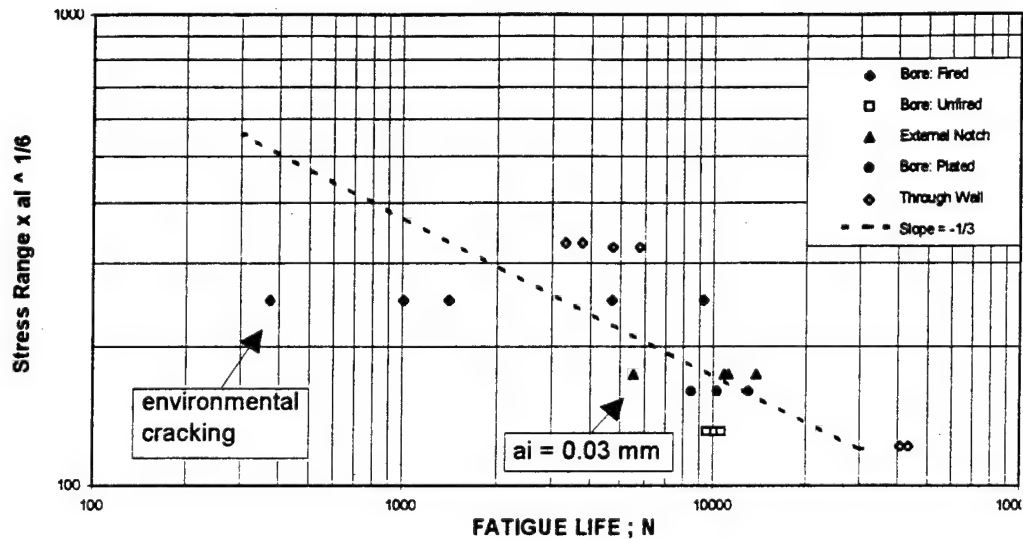


**Fig. 9 : Fatigue Life as a Function of Stress Range and Initial Crack Size**

The results plotted in Fig. 9 are in approximate agreement with a line of  $-1/3$  slope as predicted in Fig. 4. The most significant deviations from the single line plot are some of the fired tubes with bore failure, particularly the tube that failed in less than 400 cycles. In the prior work, [4], intergranular fracture was noted for this tube, and environmental cracking, often associated with intergranular fracture, was considered to be possible. In light of the results here, it appears that environmental cracking did indeed contribute to the early failure. A clear advantage of the single line analysis of fatigue results - including as it does the three important variables,  $\Delta\sigma$ ,  $N$  and  $a_i$  - is the identification of an apparent fatigue failure that has been affected by other than pure mechanical fatigue processes such as environmental cracking in the example just discussed.

Another advantage of the single line plot of fatigue results is that it provides a quantitative procedure to account for variations in  $a_i$ , which can be overlooked in a conventional  $\Delta\sigma$  -  $N$  plot. For example if the external notch result in Fig. 9 with  $a_i = 0.03$  mm had been plotted with no account of its different value of  $a_i$ , it would have increased the apparent scatter and uncertainty of the results. Accounting for  $a_i$  gives a better understanding of the fatigue life results.

A final comment on the results is that without the inclusion of the effects of residual stresses described earlier, the agreement of the results with the single line analysis would have been affected. The results from the plated tubes and those with through-wall holes would have been in poorer agreement with the other results. This shows the important effect that residual stresses can have on  $\Delta\sigma$  and thus on life.

## SUMMARY AND CONCLUSIONS

An analysis has been developed which permits fatigue lifetimes of components with pre-existing crack-like defects to be represented by a single expression which is a function of stress range and initial defect size; this is designated the *Fatigue Intensity Factor (FIF)*. Graphical representation indicates that all such failures will fall upon a single, flat surface. Outliers from this surface may indicate deficiencies in estimates of stress range, of initial crack length, or that the failure is due to other factors in addition to mechanical fatigue.

An equivalent analysis links the so-called stress intensity threshold to the fatigue limit. This gives rise to a second, intersecting flat surface. The combination of these three-dimensional surface representations is shown to be the general, fully quantified case of the conventional S-N presentation with fatigue limit.

Existing experimental data are used to define the surface, and examples of its application are indicated in a two dimensional presentation. Cannon tube fatigue life results are shown to plot on a single line when the applied and residual stresses and known variations in initial crack size are accounted for. Fatigue lives known to be affected by environmental cracking are significant outliers from the single line plot, with lives reduced by up to a factor of ten from the lives due only to mechanical fatigue.

## ACKNOWLEDGEMENT

Much of this work was undertaken during an attachment by one of the authors (APP) to the US Army Armament Research, Development and Engineering Center, Watervliet, NY. The attachment was arranged via the European Research Office of the US Army Research, Development and Standardization Group (UK).

## REFERENCES

- [1] Paris, P. C. and Erdogan, F., "A Critical Analysis of Crack Propagation Laws", Journal of Basic Engineering, Trans ASME, Vol.85, pp 528-534, 1963.
- [2] Maddox, S. J., "Assessing the Significance of Flaws in Welds Subject to Fatigue", Welding Research Supplement, American Welding Society, Vol. 53, No. 9, pp 401-409, 1974.
- [3] Gurney, T. R., "Fatigue of Welded Structures", 2nd Edition, Cambridge University Press, 1979.
- [4] Davidson, T. E., Throop, J. F. and Underwood, J. H., "Case Studies in Fracture Mechanics", AMMRC MS 77-5, Army Materials and Mechanics Research Center, Watertown MA, 1977, pp 3.9.3 - 3.9.13.
- [5] Audino, M. J., "Fatigue Life Assessment of 155-MM M284 Cannon Tubes", ARCCB-TR-93036, Army Armament Research, Development and Engineering Center Report, Watervliet, NY, 1993.
- [6] Underwood, J. H., Parker, A. P., Corrigan, D. J. and Audino M. J., "Fatigue Life Measurements and Analysis for Overstrained Tubes with Evacuator Holes", presented at ASME PVP Conference, Hawaii, 1995 and to be published in ASME Journal of Pressure Vessel Technology , 1996.
- [7] Roark, R. J. and Young, W. C., Formulas for Stress and Strain, McGraw-Hill, New York, 1975, pp 590 - 606.
- [8] Parker, A. P., "Stress Intensity and Fatigue Crack Growth in Multiply-Cracked, Pressurized, Partially Autofrettaged Thick Cylinders", Fatigue of Engineering Materials and Structures, Vol. 4, No. 4, pp 321-330, 1981.

---

TECHNICAL REPORT INTERNAL DISTRIBUTION LIST

	<u>NO. OF COPIES</u>
CHIEF, DEVELOPMENT ENGINEERING DIVISION	
ATTN: AMSTA-AR-CCB-DA	1
-DB	1
-DC	1
-DD	1
-DE	1
CHIEF, ENGINEERING DIVISION	
ATTN: AMSTA-AR-CCB-E	1
-EA	1
-EB	1
-EC	1
CHIEF, TECHNOLOGY DIVISION	
ATTN: AMSTA-AR-CCB-T	2
-TA	1
-TB	1
-TC	1
TECHNICAL LIBRARY	
ATTN: AMSTA-AR-CCB-O	5
TECHNICAL PUBLICATIONS & EDITING SECTION	
ATTN: AMSTA-AR-CCB-O	3
OPERATIONS DIRECTORATE	
ATTN: SIOWV-ODP-P	1
DIRECTOR, PROCUREMENT & CONTRACTING DIRECTORATE	
ATTN: SIOWV-PP	1
DIRECTOR, PRODUCT ASSURANCE & TEST DIRECTORATE	
ATTN: SIOWV-QA	1

NOTE: PLEASE NOTIFY DIRECTOR, BENÉT LABORATORIES, ATTN: AMSTA-AR-CCB-O OF ADDRESS CHANGES.

---

---

TECHNICAL REPORT EXTERNAL DISTRIBUTION LIST

	<u>NO. OF COPIES</u>		<u>NO. OF COPIES</u>
ASST SEC OF THE ARMY RESEARCH AND DEVELOPMENT ATTN: DEPT FOR SCI AND TECH THE PENTAGON WASHINGTON, D.C. 20310-0103	1	COMMANDER ROCK ISLAND ARSENAL ATTN: SMCRI-SEM ROCK ISLAND, IL 61299-5001	1
DEFENSE TECHNICAL INFO CENTER ATTN: DTIC-OCF (ACQUISITIONS) 8725 JOHN J. KINGMAN ROAD STE 0944 FT. BELVOIR, VA 22060-6218	2	MIAC/CINDAS PURDUE UNIVERSITY 2595 YEAGER ROAD WEST LAFAYETTE, IN 47906-1398	1
COMMANDER U.S. ARMY ARDEC ATTN: AMSTA-AR-AEE, BLDG. 3022	1	COMMANDER U.S. ARMY TANK-AUTMV R&D COMMAND ATTN: AMSTA-DDL (TECH LIBRARY) WARREN, MI 48397-5000	1
AMSTA-AR-AES, BLDG. 321	1	COMMANDER U.S. MILITARY ACADEMY ATTN: DEPARTMENT OF MECHANICS WEST POINT, NY 10966-1792	1
AMSTA-AR-AET-O, BLDG. 183	1		
AMSTA-AR-FSA, BLDG. 354	1		
AMSTA-AR-FSM-E	1		
AMSTA-AR-FSS-D, BLDG. 94	1		
AMSTA-AR-IMC, BLDG. 59	2	U.S. ARMY MISSILE COMMAND REDSTONE SCIENTIFIC INFO CENTER ATTN: AMSMI-RD-CS-R/DOCUMENTS BLDG. 4484 REDSTONE ARSENAL, AL 35898-5241	2
PICATINNY ARSENAL, NJ 07806-5000			
DIRECTOR U.S. ARMY RESEARCH LABORATORY ATTN: AMSRL-DD-T, BLDG. 305 ABERDEEN PROVING GROUND, MD 21005-5066	1	COMMANDER U.S. ARMY FOREIGN SCI & TECH CENTER ATTN: DRXST-SD 220 7TH STREET, N.E. CHARLOTTESVILLE, VA 22901	1
DIRECTOR U.S. ARMY RESEARCH LABORATORY ATTN: AMSRL-WT-PD (DR. B. BURNS) ABERDEEN PROVING GROUND, MD 21005-5066	1	COMMANDER U.S. ARMY LABCOM, ISA ATTN: SLCIS-IM-TL 2800 POWER MILL ROAD ADELPHI, MD 20783-1145	1
DIRECTOR U.S. MATERIEL SYSTEMS ANALYSIS ACTV ATTN: AMXSY-MP ABERDEEN PROVING GROUND, MD 21005-5071	1		

NOTE: PLEASE NOTIFY COMMANDER, ARMAMENT RESEARCH, DEVELOPMENT, AND ENGINEERING CENTER,  
BENÉT LABORATORIES, CCAC, U.S. ARMY TANK-AUTOMOTIVE AND ARMAMENTS COMMAND,  
AMSTA-AR-CCB-O, WATERVLIET, NY 12189-4050 OF ADDRESS CHANGES.

---

# TECHNICAL REPORT EXTERNAL DISTRIBUTION LIST (CONT'D)

	<u>NO. OF COPIES</u>		<u>NO. OF COPIES</u>
COMMANDER U.S. ARMY RESEARCH OFFICE ATTN: CHIEF, IPO P.O. BOX 12211 RESEARCH TRIANGLE PARK, NC 27709-2211	1	WRIGHT LABORATORY ARMAMENT DIRECTORATE ATTN: WL/MNM EGLIN AFB, FL 32542-6810	1
DIRECTOR U.S. NAVAL RESEARCH LABORATORY ATTN: MATERIALS SCI & TECH DIV WASHINGTON, D.C. 20375	1	WRIGHT LABORATORY ARMAMENT DIRECTORATE ATTN: WL/MNMF EGLIN AFB, FL 32542-6810	1

NOTE: PLEASE NOTIFY COMMANDER, ARMAMENT RESEARCH, DEVELOPMENT, AND ENGINEERING CENTER,  
BENÉT LABORATORIES, CCAC, U.S. ARMY TANK-AUTOMOTIVE AND ARMAMENTS COMMAND,  
AMSTA-AR-CCB-O, WATERVLIET, NY 12189-4050 OF ADDRESS CHANGES.

---